Propylene/Propane Separation by Vacuum Swing Adsorption Using 13X Zeolite

Francisco A. Da Silva and Alírio E. Rodrigues
Laboratory of Separation and Reaction Engineering, Dept. of Chemical Engineering, University of Porto, 4200-465 Porto, Portugal

A vacuum swing adsorption process using 13X zeolite pellets with five steps was designed to split an equimolar mixture of propylene/propane: pressurization with feed; high-pressure feed; high-pressure purge with product; cocurrent blowdown; and countercurrent vacuum blowdown, where the enriched propylene product is withdrawn. In the process, the partial pressure of the C_3-mixture is controlled with nitrogen, which is used as inert gas. With an equimolar feed of C_3 diluted to 50% with nitrogen, the column is fed at 5 bar and 423 K, and the product is obtained when the total pressure is lowered to 0.1 bar. After 15–20 cycles, the cyclic steady-state condition is achieved, a propylene-enriched stream of 98% mol relative to propylene/propane mixture, with 3.2% of nitrogen, a recovery of 19% (molar basis), and a productivity of 0.785 mol/kg · h is obtained. The experimental work was complemented with numerical simulations, and the effect of different operating parameters on the performance of the VSA was considered.

Introduction

The propylene/propane separation by distillation to produce polymer-grade propylene (99.8–99.9+% purity) is difficult because the relative volatility for this system is between 1.0 and 1.1 at temperatures in the range of 244–327 K and total pressure of 1.7–22 bar (Manley and Swift, 1971). This makes the propylene/propane one of the most energy-expensive separations in the petrochemical industry (Eldridge, 1993). Polymer-grade propylene is obtained through a C_3 splitter column system with more than 200 trays typically built in a two-column arrangement (Sherred and Fair, 1959; Smuck, 1963; Tyreus and Luyben, 1975; Finelt, 1979; Howat and Swift, 1980; Summers et al., 1995; Netzer, 1997). The columns are 75–90 m tall and have 2–6 m diameter, and work with a high reflux ratio (15–25) and a tray efficiency between 70 and 80%.

Physical/chemical adsorption appears to be the most attractive alternative, because of the maturity of the technology, the available adsorbents, and low-cost, low-energy but highly efficient gas separation system (Wiessner, 1988). Hybrid methods that combine the traditional distillation and adsorption processes have been proposed as an economical alternative (Kumar et al., 1992; Ghosh et al., 1993; Eldridge, 1993). The basic idea is to carry out the most difficult separation (paraffin/olefins) with adsorption, and further improvement with distillation, such as the energy-intensive and expensive olefin–alkane distillation, is eliminated (Kumar et al., 1992).

Recent efforts to find and characterize the available sorbents and produce new sorbents to carry out the propylene/propane separation via vacuum swing adsorption have appeared in the literature (Kubota et al., 1989; Loughlin et al., 1990; Costa et al., 1991; Järvelin and Fair, 1993; Ghosh et al., 1993; Huang et al., 1994; Yang and Kikkinides, 1995; Da Silva and Rodrigues, 1999a). In general, the available sorbents have higher selectivity for propylene. The PSA operation is then constrained to produce propylene during the blowdown step, and preferably in vacuum countercurrent blowdown (VSA) due to the high favorable character of the

Correspondence concerning this article should be addressed to A. E. Rodrigues.
Present address of F. A. Da Silva: Department of Chemistry, University of Aveiro, 3810-193, Aveiro, Portugal.

adsorption of propylene isotherm. The other option is to work with a temperature swing adsorption unit (TSA).

The following methods have been used to carry out the propylene/propane separation in an equilibrium controlled regime:

Variable-Temperature Stepwise Desorption. Kulvaranon et al. (1990) showed a method called variable-temperature stepwise desorption (VTSD) process based in the TSA concept with the following steps. (1) load step: The propylene/propane mixture is fed at 25°C and 1–1.33 atm until the column is completely saturated. (2) Desorption programmed step: The external oil bath temperature of the column is increased following a ramp program policy from 50°C to 160°C, allowing the flow to exit at constant column pressure (1 atm), until propylene is completely depleted (propylene production). From a binary mixture of C_3H_6/C_3H_8 25/75, a product with 85% purity is obtained using 13X and 5A zeolites. They carried out an economic comparison between adsorption–VTSD and distillation assuming a total cycle time of 1.5 h, demonstrating that distillation capital investment is lower while the distillation energy costs are higher. They suggested that the adsorption of the high-concentration component for purification is not likely to be economically competitive, since the amount of adsorbent is very large compared to the total amount of the mixture processed in the separation. For this reason they concluded that adsorption is more cost competitive when low concentration components are adsorbed for recovery and further separation compared with the amounts adsorbed. This explains why a low purity of 85% is attractive for applying their separation procedure, with the objective of recovering the olefins from the effluent of a catalytic cracking operation. A similar idea has been patented by Ramachandran et al. (1998) from BOC, but they proposed not only the TSA to recover the olefins, but the PSA or a combination of both processes to carry out the same task.

TSA With Nitrogen Hot Purge. Järvelin and Fair (1993) proposed a three-stage adsorption procedure to carry out the propylene/propane separation. The first adsorption/desorption unit is a TSA system constituted by two steps: (1) low-temperature loading until saturation with the propylene/propane mixture diluted with nitrogen (propane production); and (2) high-temperature purge with nitrogen (propylene production). The nitrogen/propane and nitrogen/propylene products streams are then each separated into a second stage by adsorption using activated carbon in another two-step TSA unit. The adsorption step, which lasts 100 min, is at 25°C, 269 kPa with a feed of propylene/propane 1.162%/1.185% mol balanced with nitrogen; which takes the purge step, with nitrogen is at 200°C, 269 kPa, takes 100 to 200 min with the sorbents 4A, 5A, or 13X zeolite. After the first 10 min, the product stream in this second step is pure propylene in nitrogen, and the total cycle time is between 200 and 300 min. Supported by this information, a three-step TSA system for carrying out the first-stage separation was studied (Da Silva and Rodrigues, 1999b). The system is able to split the propylene/propane effectively; however, the product obtained is too diluted in nitrogen and requires a large recycle stream (Järvelin and Fair, 1993).

Vacuum Swing Adsorption. Kumar et al. (1992) proposed a 4-bed 5-step VSA process for performing the propylene/propane splitting as follows. (1) Pressurization: with a mixture of C_2H_6 and C_2H_8 from another VSA unit that is working in parallel separating H_2/CH_4 from $H_2/CH_4/C_2H_6/C_3H_8$. (2) High-pressure feed: the raffinate from this stream ($H_2/CH_4/C_2H_6/C_3H_8$) is sent to another VSA system where the H_2/CH_4 stream is produced. (3) Cocurrent depressurization to an intermediate pressure. (4) Cocurrent purge with propylene product. (5) Countercurrent blowdown (propylene production). The duration of each step is between 1 and 10 min. The low-pressure purge with propylene product is at atmospheric pressure, the total high-pressure is between 4 and 5 bar with a high amount of H_2, and the cocurrent and pressurization steps could spend about 1 m each.

Ramachandran et al. (1994) proposed a pair of column adsorption vessels, each with a heating jacket with 3.84 kg of 4A zeolite and implemented the following adsorption cycle: (1) countercurrent pressurization with nonadsorbed product (7 s); (2) high-pressure feed (34 s); (3) bed equalization (9 s); (4) countercurrent depressurization (41 s); (5) bed equalization (9 s). The total time cycle is 100 s and operates between $P_H = 1.7$-bar and $P_M = 0.7$-bar pressure equalization, and then evacuates between 0.2 and 0.1 bar (P_L). From a feed of propylene/propane 88/12, at 90°C, with 4A zeolite, a purity of 96% and a recovery of 97% were obtained, with productivity of 1.2 mol/kg·h, and the steady-state conditions were reached after more than 100 cycles. Ramachandran et al. found that at low temperature (30–70°C), propane rejection is poor, which was confirmed numerically by Da Silva et al. (1996). They also found that, in terms of recovery of propylene the performance was worse with 13X zeolite (purity 90%, recovery 88%, and productivity 1.9 mol/kg·h, respectively). While propane behaves as inert gas in 4A zeolite, it is adsorbed in 13X zeolite, and therefore a purge step to obtain high-purity product is required. Sikavitsas et al. (1995) and Rege et al. (1998) carried out numerical simulations of a four-step VSA process for performing the propylene/propane splitting with the following steps: (1) pressurization with feed; (2) high-pressure feed with fresh feed and recycle high-pressure purge product; (3) high-pressure purge with high-purity olefin product; (4) countercurrent vacuum blowdown (propylene production). The stream exiting during the cocurrent high-pressure purge in this four-step VSA is recycled and mixed with the fresh feed to be processed. This process allows the complete saturation of the column in the cocurrent purge step until the propylene breakthrough, which will be recycled. Yang and coworkers (Yang and Kikkinides, 1995; Yang et al., 1996; Padin and Yang, 1997) have been researching new sorbents for the paraffin/olefin separation based on the "π-complexation" phenomena. They showed that a new sorbent prepared with ion-exchanged resins (Amberlyst 15 and, more recently, Amberlyst 35), with Ag^+, and $CuCl/\gamma-Al_2O_3$, has appropriate loading and selectivity for performing C_2H_4/C_2H_6 and C_3H_6/C_2H_8 gas splitting. For the propylene/propane system, the main difficulty with the new sorbents has been the mass-transfer resistance, which restricts the performance of the sorbent when used during the VSA operation. Sikavitsas et al. (1995) tried to reduce the mass-transfer resistance problem, by simulating a PSA with a magnetic stabilized bed (MSB), that is, the resin-Ag^+ is suspended during the high-pressure feed step by a magnetic field. The advantage of this bed operation is that it reduces mass-

transfer resistance, because the suspended-expanded bed during the adsorption step allows the operation with small sorbent particles. Sikavitsas et al. performed the simulations, splitting a C_3H_8/C_3H_6 58/42 feed operating between 1 and 0.03 atm at 298 K and obtained a product purity higher than 98% and a recovery of over 15% with the MSB-VSA, while recoveries lower than 1% with 99% of purity were obtained using the conventional 4-step VSA. Higher recovery (10%) with a similar purity was obtained by Da Silva and Rodrigues (1999b) in their numerical simulations with the same VSA cycle, but using smaller particles with higher vacuum pressure ($P_L = 5$ kPa) and larger pressure drops along the column. Rege et al. (1998) presented improved theoretical predictions using the same VSA cycle with a $AgNO_3/SiO_2$ sorbent. They also used a 4A zeolite to compare with the VSA performance. Operating at higher temperatures (70°C with the $AgNO_3/SiO_2$ and 100°C with the 4A zeolite rather than 25°C as with resin-Ag^+), the simulated results with both sorbents led to product purities between 98 and 99% and recoveries between 20 and 40% with the new $AgNO_3/SiO_2$ working at 70°C, while with 4A zeolite the purities were over 99%, always with recoveries between 8 and 27%, at 100°C.

The aim of this work is to develop through simulation and experiments a new 5-step vacuum swing adsorption process to produce high-purity propylene from an equimolar propane/propylene mixture, using a 13X commercial zeolite.

Experimental Setup

The experimental setup is shown in Figure 1. It contains five main sections:

1. The *mixture section* consists of three mass-flow controllers, MFC1, MFC2, and MFC3, connected to nitrogen, propylene, and propane cylinders. The three flowmeters are from Teledyne (VA), models HFC-202 are the MFC1 calibrated for nitrogen (0–5 SLPM), propylene (0–2 SLPM), and propane (0–2 SLPM) with a linear response between 0 and 5 VDC, with an error lower than 0.5% in the flow scale.

2. The *VSA/PSA column section* consists of a convective air furnace, five solenoid valves, two check valves, a pressure transducer, three thermocouples, and the column. The furnace is from Thermolab (Águeda, Portugal) and is equipped with 3 2116 Eurotherm PID controllers (Reston, VA), 2 Siemens 50CV motors, 12 1250-W 220-V resistances, which allow controlled temperatures between 30 and 400°C (±1°C with the turbines on). The solenoid valves are normally closed; they open with a 24-V input (13 W), from Flo-Control (Milan, Italy) model Q2C124, and can handle gas or liquid mixtures up to 70°C and support back pressure up to 5 bar. The two check valves are Parker C-Series (UK) model 4A-C4L-1SS. The pressure transducer PT1 is Lucas (Slough, UK) model P4163-0005-0007BA, with linear pressure response from 0 to 7 bar. The three thermocouples are K type, model KSS-M15G-600, from OMEGA (Leicestershire, UK). The column is made of inox steel 316, and is 0.8 m high and has an ID of 1.6 cm, with the three thermocouples located at 20, 40, and 60 cm from the feed end.

3. The *pressure-regulation section* consists of a back-pressure regulator, vacuum pump, a relief valve, a check valve, and two electrovalves. The back-pressure regulator is from Bronkhorst High-Tech (Ruurlo, Holland) (model P-502C-FA-020A) working between 0 and 5 bar, with 0.5% accuracy and a maximum working temperature of 70°C. The vacuum pump is from KNF (Neugberger, Germany), model N813.3 ANE diaphragm type, allowing ultimate pressure of 3 mbar and flow of up to 13 SLPM. The two solenoid valves and the check valves in this section have the same characteristics of those in paragraph 2. The relief valve is Ham-let (Migdal-Haemek, Israel) model H900SSL, working between 0 and 1540 relative kPa. This relief valve is fixed at near atmospheric pressure in order to prevent the vacuum pump from receiving input flows with higher pressure that can damage it.

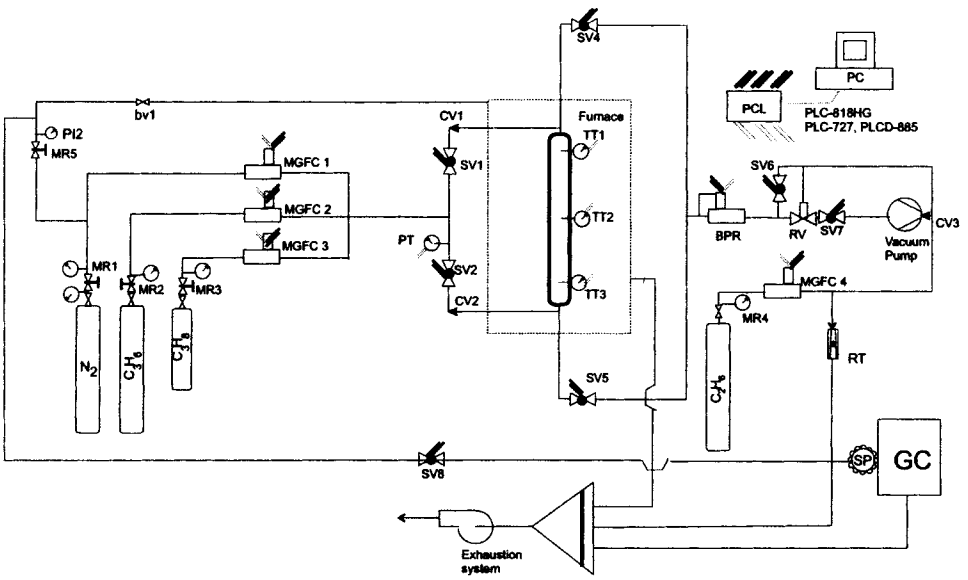

Figure 1. Apparatus of the laboratorial unit.

4. The *analytical section* includes a gas chromatograph (GC) with an automatic valve sample system, a solenoid valve, a mass-flow controller, and a computer with a data-acquisition system. This section is dedicated to controlling the cycle operation of the system and to analyzing on-line the composition of mixtures exiting the system. The computer has a QDI motherboard (Quarry Bay, Hong Kong) and an Intel Pentium 200-Mhz processor working with the Windows 95 operating system. The acquisition cards are from Advantech (Shing-Tien, Taiwan) and consist of PCL818HG, PCL727, and PCLD885 boards. The acquisition software used is Genie PCLS902, version 2.12, provided by Advantech. The gas-chromatograph system is Chrompack CP9001 (Delft, Holland), with a FID detector, and a GS-AL P/N 115-3532 wide-bore column with a 30-m × 0.53-mm ID from J&W Scientific (Folsom, CA) was used for the propylene/propane mixtures. The GC is coupled with an automatic valve sample system from Valco (Houston, TX), including the E2CST12P 12-valve model, with an electric actuator and a A4C6UWE switching valve. The loops are 10 μL each. The multiport valve is actuated through the serial valve interface SVI from Valco via an RS-232 port, and the chromatographic analysis is performed with the Maestro I v 2.4 software provided by Chrompack. In this section there is also a solenoid valve that controls a diluting nitrogen stream and a mass-flow controller model HFC-202 from Teledyne (VA) with a 0–1750 SLPM for ethane that is used as external reference flow in the gas-chromatographic analysis.

5. The *exhausting section* consists of an extractor arm and a suction pump. The extractor arm is from Alsident, System 50 + 75 HMS (Hammel, Denmark), and the suction pump is a KRJ-160-CBM-2 from Soler & Palau (Barcelona, Spain). The suction capacity of the system is 495 m^3/h under standard conditions.

All pipes are inox stainless steel of one-quarter-inch diameter from Sandvik (Sandviken, Sweden), and all connections are from Swagelok (Solon, OH), except the solenoid, relief, and check valves, which came with Ham-Let fittings (Migdal-Haemek, Israel). The interior of the convective furnace can be filled with nitrogen or with another inert gas.

Five-Step Vacuum Swing Adsorption for Separating the Propylene/Propane Mixture

The propylene/propane separation by adsorption over 13X zeolite is based on the equilibrium selectivity of propylene over propane, $\$_{propylene,propane} = 10$. The strongly adsorbed component is the target product, and so a high-pressure purge and a vacuum countercurrent blowdown will be required to obtain high-purity propylene.

A five-step VSA was designed for the propylene/propane separation with the objective of producing high-purity propylene as follows:

Step 1: *Pressurization with Feed.* The pressure is increased from the lower pressure P_L to the maximum pressure P_H with feed. This step was fixed in 60 s to raise the pressure from 0.1 bar to 5 bar with a total volumetric flow of 2 SLPM, 25% propylene, 25% propane, and 50% nitrogen, from the bottom to the top of the column.

Step 2: *High-Pressure Feed.* In this step the feed is kept at the higher pressure P_H entering the column. The bed accumulates propylene in the solid phase, and an enriched propane stream diluted with nitrogen is produced.

Step 3: *High-Pressure Purge with Product.* Part of the product is compressed, recycled, diluted with nitrogen, and introduced again in the column from the bottom to the top. This step has the objective of improving the propylene purity of the product, but at the cost of lowering the recovery of the overall system.

Step 4: *High-Pressure Cocurrent Blowdown.* During this step the column pressure is lowered to an intermediate pressure P_M. This step further enriched the gas phase, with propylene being desorbed from the solid phase, and removed the excess of nitrogen and some propane remaining in the column.

Step 5: *Low-Pressure Countercurrent Blowdown.* The pressure is lowered further from the intermediate pressure P_M to the lower pressure P_L in countercurrent. This is the production step, where high-purity propylene is obtained.

This cycle sequence shares common points with the 4-step VSA process in producing the strong adsorbed component, used by Kikkinides et al. (1993) to recover CO_2 from flue gas and more recently by Sikavitsas et al. (1995) and Rege et al. (1998) to produce propylene. However, there are the following differences. (1) The introduction of inert gas, N_2, as a purge gas, combined with part of the high-purity propylene product, during the high-pressure purge and the additional cocurrent blowdown to withdraw the inert purge excess gas. The idea of introducing an inert gas to desorb the light component is known as "purge gas stripping" (Ruthven, 1984). Sircar (1988) also used an inert purge gas (N_2) to separate "CH_4/CO_2" by producing more of the less adsorbed component, CH_4. Ramachandran et al. (1994) suggests the use of nitrogen as the stripping gas and/or propylene product, although they do not provide further details, while Seery (1999) uses a high-volume air rinse rather than pressure reduction to recover CO_2 (strongly adsorbed component) from CH_4. In the hybrid flow diagram of the olefin separation proposed by Kumar et al. (1992), H_2 is obtained as the light component. Part of this H_2 could be recycled to be used as the inert gas of the VSA in place of the nitrogen used here, if the economics of the process were favorable. (2) In the VSA of Rege et al. (1998), the stream exiting the high-pressure purge step is recycled and mixed with the high-pressure feed stream, allowing complete bed saturation during the high-pressure purge and breakthrough from the column. This recycle can also be incorporated in our cycle, for example, the fresh feed could be combined with the nonadsorbed product of the other column performing the purge step. This recycling can be carried out experimentally using at least a reservoir tank to keep the exiting stream of step 3 in the one-column operation; a two-column arrangement, or three columns (column one in feed, column two in purge step, and the third column in vacuum blowdown, producing the high product propylene, with part of the stream being compressed and recycled to two column).

Performance criteria of VSA process

The definition of the performance criteria that characterized the VSA experiments provides a common basis for comparing the different experiments. They are:

- Purge-to-feed ratio:

$$P/F = \frac{\text{Amount of } C_3H_6 \text{ used during the purge step}}{\text{Amount of } C_3H_6 \text{ fed during pressurization} + \text{amount of } C_3H_6 \text{ used in feed step}}. \quad (1)$$

- Purity:

$$\%\ \text{Purity} = \frac{(\text{Amount of } C_3H_6 \text{ obtained during blowdown step}) \times 100}{\text{Amount of } C_3H_6 + \text{amount of } C_3H_8 \text{ obtained in blowdown step}}. \quad (2)$$

- Recovery:

$$\%\ \text{Recovery} = \frac{(C_3H_6 \text{ obtained in blowdown} - C_3H_6 \text{ used in purge step}) \times 100}{C_3H_6 \text{ fed during pressurization} + C_3H_6 \text{ used in feed step}}. \quad (3)$$

- Productivity:

$$\text{Productivity} = \frac{C_3H_6 \text{ obtained in blowdown} - C_3H_6 \text{ used in purge step}}{\text{Total sorbent mass} \times \text{total cycle time}}. \quad (4)$$

Mathematical Model

The mathematical model used in the simulations is shown in Table 1. It is a bidisperse mass-transfer control model, with a heterogeneous energy balance with local pressure drop following the Ergun's correlation. The isotherm used is the Toth extended model (Sircar, 1991), while the axial dispersion groups $\epsilon D_{zm,i}/D_{m,i}$, λ/k_g, and the Sherwood and Nusselt numbers, $K_{m,i}d_p/D_{m,i}$ and $h_f d_p/k_k$, respectively, are calculated with the Wakao and Funazkri (1978) correlations, as suggested by Yang (1987). All properties in the bulk gas phase, that is, viscosity, thermal gas conductivity, and molecular diffusion, are calculated with the reference conditions and then corrected locally by temperature and pressure according to Lu et al. (1993). The boundary conditions for the pressurization, high-pressure feed, high-pressure purge, cocurrent blowdown, and countercurrent blowdown are shown in Table 2. During the pressurization/depressurization steps, an exponential valve equation type is used following the experimental data (Lu et al., 1993; Rege et al., 1998). For fixed-bed runs, the boundary conditions are the same as the high-pressure feed/purge steps, which are equivalent to Danckwerts' boundary conditions. As the initial condition, inert gas flowing isothermically through the column is used before the fixed bed and during the first pressurization step in cycle operation. For the cyclic process the earlier conditions at the end of the last cycle are the initial condition of the new cycle.

The set of partial differential equations is solved with the method of lines (Schiesser, 1991) using the orthogonal collocation of finite elements (Carey and Finlayson, 1975), shifted Jacobi polynomials calculated with Villadsen and Michelsen (1978) routines, and the resulting set of differential-algebraic equations (DAE) solved with the DASPK library. The code was implemented in a general-purpose numerical package called SAXS (Da Silva and Rodrigues, 1999b); further details can be found elsewhere (Da Silva, 1999).

Table 1. Mathematical Model Solved with SAXS Package to Simulate the VSA Process

Overall mass balance	$\epsilon\frac{\partial C}{\partial t} = -\frac{\partial (uC)}{\partial z} - \sum_{i=1}^{n} N_i$
Component mass balance	$\epsilon\frac{\partial C_i}{\partial t} = \frac{\partial}{\partial z}\left(\epsilon D_{zm,i} C \frac{\partial Y_i}{\partial z}\right) - \frac{\partial (uC_i)}{\partial z} - N_i$
Ergun's equation	$-\frac{\partial P}{\partial z} = \frac{150\mu(1-\epsilon)^2}{\epsilon^3 d_p^2}u + \frac{1.75(1-\epsilon)\rho}{\epsilon^3 d_p}\lvert u\rvert u$
Mass transfer rate to solid	$N_i = (1-\epsilon)\frac{aK_{m,i}}{Bi_{m,i}+1}(C_i - \bar{c}_i)$
	$\frac{\partial \bar{c}_i}{\partial t} = \frac{15\bar{D}_{p,i}}{R_p^2}\frac{Bi_{m,i}}{(Bi_{m,i}+1)}(C_i - \bar{c}_i)\frac{\rho_p w_c}{\epsilon_p}\frac{\partial \bar{\bar{n}}_i}{\partial t}$
	$\frac{\partial \bar{\bar{n}}_i}{\partial t} = \frac{15\bar{D}_{c,i}}{r_c^2}(n_i^* - \bar{\bar{n}}_i)$
Gas energy balance	$\epsilon C\bar{C}_v\frac{\partial T_g}{\partial t} = \frac{\partial}{\partial z}\left(\lambda\frac{\partial T_g}{\partial z}\right) - uC\bar{C}_p\frac{\partial T_g}{\partial z} + \epsilon\Re T_g\frac{\partial C}{\partial t}$
	$-(1-\epsilon)ah_f(T_g - T_s) - \frac{2h_w}{R_w}(T_g - T_w)$
Solid energy balance	$(1-\epsilon)\left\{\epsilon_p\sum_{i=1}^{n}\bar{c}_i\tilde{C}_{v,i} + \rho_p w_c\sum_{i=1}^{n}\bar{\bar{n}}_i\tilde{C}_{v,ads,i} + \rho_p\hat{C}_{ps}\right\}$
	$\times\frac{\partial T_s}{\partial t} = (1-\epsilon)\epsilon_p\Re T_s\frac{\partial \bar{c}}{\partial t} + \rho_b w_c\sum_{i=1}^{n}$
	$\times(-\Delta H_i)\frac{\partial \bar{\bar{n}}_i}{\partial t} + (1-\epsilon)ah_f(T_g - T_s)$
Wall energy balance	$\rho_w\hat{C}_{pw}\frac{\partial T_w}{\partial t} = \alpha_w h_w(T_g - T_w) - \alpha_{w\ell}U(T_w - T_\infty)$
Toth's extended equation	$n_i^* = \frac{mb_i\bar{c}_i\Re T_s}{\left(1+\sum_{i=1}^{n}(b_i\bar{c}_i\Re T_s)^k\right)^{1/k}}$
Mass axial-dispersion term	$\frac{\epsilon D_{zm,i}}{D_{m,i}} = 20 + 0.5Sc_i Re$
Heat axial-dispersion term	$\frac{\lambda}{k_g} = 7 + 0.5PrRe$
Mass-transfer coefficient	$\frac{K_{m,i}d_p}{D_{m,i}} = 2.0 + 1.1Re^{0.6}Sc_i^{1/3}$
Heat-transfer coefficient	$\frac{h_f d_p}{k_g} = 2.0 + 1.1Re^{0.6}Pr^{1/3}$

Fixed-Bed Experiments

Breakthrough experiments were performed before the VSA runs in order to review the behavior of the new equipment and to fix operational restrictions for the VSA to be considered next.

Table 2. Boundary Conditions

Step I: Pressurization

z = 0	z = L
$P(t)\|_{z^+} = P(0)\|_{z^+} + (P(t_I)\|_{z^-} - P(0)\|_{z^+})[1-\exp(-M_a t_I)]$	$u\|_{z^-} = 0$
$-\epsilon D_{zm,i} C \left.\frac{\partial Y_i}{\partial z}\right\|_{z^+} + uC_i\|_{z^+} - uC_i\|_{z^-} = 0$	$\left.\frac{\partial Y_i}{\partial z}\right\|_{z^-} = 0$
$-\lambda \left.\frac{\partial T_g}{\partial z}\right\|_{z^+} + uC\tilde{C}_{pg} T_g\|_{z^+} - uC\tilde{C}_{pg} T_g\|_{z^-} = 0$	$\left.\frac{\partial T_g}{\partial z}\right\|_{z^-} = 0$

Steps II and III: High-Pressure Feed and Purge

z = 0	z = L
$Cu\|_{z^+} = Cu\|_{z^-}$	$P\|_{z^-} = P\|_{z^+}$
$-\epsilon D_{zm,i} C \left.\frac{\partial Y_i}{\partial z}\right\|_{z^+} + uC_i\|_{z^+} - uC_i\|_{z^-} = 0$	$\left.\frac{\partial Y_i}{\partial z}\right\|_{z^-} = 0$
$-\lambda \left.\frac{\partial T_g}{\partial z}\right\|_{z^+} + uC\tilde{C}_{pg} T_g\|_{z^+} - uC\tilde{C}_{pg} T_g\|_{z^-} = 0$	$\left.\frac{\partial T_g}{\partial z}\right\|_{z^-} = 0$

Step IV: Cocurrent Blowdown

z = 0	z = L
$u\|_{z^+} = 0$	$P(t)\|_{z^-} = P(0)\|_{z^-} + [P(t_{IV})\|_{z^+} - P(0)\|_{z^-}][1-\exp(-M_b t_{IV})]$
$\left.\frac{\partial Y_i}{\partial z}\right\|_{z^+} = 0$	$\left.\frac{\partial Y_i}{\partial z}\right\|_{z^-} = 0$
$\left.\frac{\partial T_g}{\partial z}\right\|_{z^+} = 0$	$\left.\frac{\partial T_g}{\partial z}\right\|_{z^-} = 0$

Step V: Countercurrent Blowdown

z = 0	z = L
$P(t)\|_{z^+} = P(0)\|_{z^+} + [P(t_V)\|_{z^+} - P(0)\|_{z^+}][1-\exp(-M_c t_V)]$	$u\|_{z^-} = 0$
$\left.\frac{\partial Y_i}{\partial z}\right\|_{z^+} = 0$	$\left.\frac{\partial Y_i}{\partial z}\right\|_{z^-} = 0$
$\left.\frac{\partial T_g}{\partial z}\right\|_{z^+} = 0$	$\left.\frac{\partial T_g}{\partial z}\right\|_{z^-} = 0$

Two basic steps belonging to the standard VSA cycle are covered in the fixed-bed experiments: (1) the high-pressure feed at 1.1, 2 and 5 bar (the loading step), and (2) the blowdown steps in countercurrent from the higher pressure to 0.1 bar (regeneration or production step). The oven temperature was fixed at 423 K for the first eight runs and at 393 K for the last two runs. Table 3 shows the operating conditions of the completed experiments, while Table 4 shows the bed and adsorbent characteristics, as well as the physical properties of the mixtures used in the fixed-bed experiments and the VSA runs. The equilibrium isotherm of single-component and macropore porosity were determined by independent experiments (Da Silva and Rodrigues, 1999a). The wall heat film transfer coefficient h_w and the overall heat-transfer coefficient U were optimized for the convective furnace from runs A–C and then fixed for the rest of the simulations.

The experiments are carried out in two consecutive steps: first, the column is filled with nitrogen and then fed with an equimolar propylene/propane mixture diluted with nitrogen at approximately 50%; second, a countercurrent blowdown is carried out. In runs A, B, and C only the high-pressure feed was done, while the blowdown step was incorporated in the last group of experiments (from D to I). Temperatures recorded at 20, 40, and 60 cm at the feed end and the mole concentration of propylene (closed circles) and propane (open circles) exiting the column are shown in Figure 3 for the high-pressure feed step and countercurrent blowdown from 5 bar to 0.1 bar at 423 K, with the flow conditions of Run G (Table 3). The solid lines represent model predictions with SAXS, with the operating parameters given in Table 4 using the model equations shown in Table 1.

During the high-pressure feed step, we observed the characteristic overshoot of the propane breakthrough being displaced by the most adsorbed component, propylene. After the loading of the column, the countercurrent blowdown begins, and during the pressure-reduction, propylene concentration is still higher than propane, as observed in Figure 3; however, the propane concentration in this step is significant, suggesting that a single vacuum blowdown step is not enough to produce high-purity propylene from 13X zeolite. In the same experiment, the temperature increases 30 K in the feed step, while it decreases nearly 15 K during the pressure reduction as a consequence of the endothermic behavior of the desorption step. This asymmetry of the temperature history reveals the nonlinear behavior of the isotherm that rules the adsorption/desorption steps of the propylene/propane system over 13X CECA zeolite. Also, it can be seen by comparing the temperature history at the three thermocouples inside the column during the feed step, that the two temperature peaks appear at the middle and at the end of the column (see Figures 3e and 3g). Each peak corresponds approximately to one mass-transfer zone, the faster one to

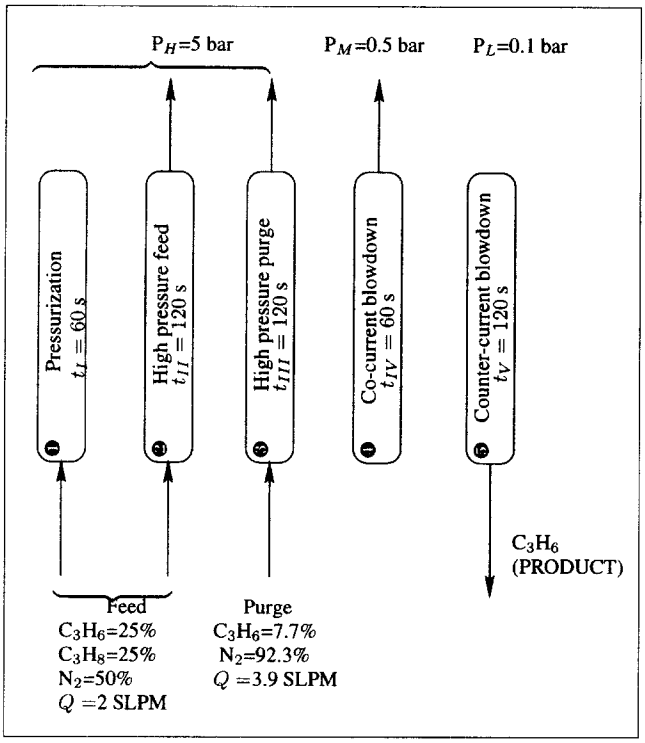

Figure 2. Five-step VSA process for separating C_3H_6/C_3H_8.

Base operating parameters for run 13 with 13X zeolite. Furnace temperature, 423 K.

propane being readsorbed in the column, and the slower one to the displacement of propane by propylene, which is the more adsorbed compound. SAXS predicts both peaks during the adsorption step at the three locations of the thermocouples, while in the experimental runs it is difficult to differentiate both peaks at the first thermocouple position (see Figure 3a). This shows a limitation in the experimental setup, which is not fast enough to detect this tiny difference. In the blowdown step, those temperature fronts are not observed and the temperature evolution in the three thermocouples is approximately the same. No clear mass-transfer zones are produced during the blowdown step as a consequence of the dispersive behavior of the desorption process.

Table 3. Operating Conditions of Fixed-Bed Experiments with Propylene/Propane over 13X CECA Zeolite

Run	T (K)	P (bar)	$Q_{propylene}$ (SCCM)	$Q_{propane}$ (SCCM)	$Q_{nitrogen}$ (SCCM)
A	423	5	450	600	1,100
B	423	5	450	600	1,100
C	423	5	450	600	1,100
D	423	1.1	450	600	1,100
E	423	5	0	500	1,750
F	423	5	500	0	1,750
G	423	5	500	500	1,000
H	423	2	500	500	1,000
I	393	5	500	500	1,000
J	393	5	250	250	500

Table 4. Adsorption-Bed Characteristics, Physical Properties for $C_3H_6/C_3H_8/N_2$ System over 13X CECA Zeolite

Column	
Bed radius (R_w)	0.008 m
Bed length (L)	0.80 m
Bed porosity (ϵ)	0.49
Bulk density (ρ_b)	690 kg/m^3
Wall density (ρ_w)	8,238 kg/m^3
Wall heat capacity ($\hat{C}_{pw}$)	500 J/kg·K
Wall heat film transfer coefficient (h_w)	60 W/m^2·K
Overall heat-transfer coefficient (U)	30 W/m^2·K
Adsorbent: 13X CECA extrudates	
Crystal radius (r_c)	1.0 μm
Pellet length	5 mm
Pellet radius (R_p)	0.8 mm
Pellet density (ρ_p)	1,357 kg/m^3
Pellet void fraction (ϵ_p)	0.39
Tortuosity (τ)	2.2
Solid heat capacity ($\hat{C}_{ps}$)	920 J/kg·K
Equilibrium	$n_i^* = \dfrac{mb_i\bar{c}_i\Re T_s}{\left(1+\sum_{i=1}^{n}(b_i\bar{c}_i\Re T_s)^k\right)^{1/k}}$
Affinity equilibrium parameter (b_i)	$b_i = b_{i,o}\exp(-\Delta H_i/\Re T)$
Component	$b_{i,o}$, kPa^{-1} — $-\Delta H_i$, kJ/mol
propylene	3.5×10^{-7} — 42.4
propane	5.0×10^{-7} — 35.8
Heterogeneity parameter (k)	0.6
Loading saturation coefficient (m)	2.67 mol/kg
Gas reference parameters	
Reference temperature (T_o)	423 K
Reference pressure (P_o)	1.01 bar
Gas viscosity (μ_o)	1.5×10^{-5} kg/m·s
Gas thermal conductivity (k_{go})	2.9×10^{-2} W/m·K
Molecular bulk diffusion ($D_{m,i,o}$)	
propylene	1.8×10^{-5} m^2/s
propane	1.7×10^{-5} m^2/s
nitrogen	2.2×10^{-5} m^2/s
Gas heat capacity	$\tilde{C}_{p,i} = \sum_{i=0}^{3}\alpha_i T^i$

Component	α_0 (J/mol·K)	α_1 (J/mol·K^{-1})	α_2 (J/mol·K^{-2})	α_3 (J/mol·K^{-3})
propylene	3.71	2.35×10^{-1}	-1.16×10^{-4}	2.21×10^{-8}
propane	−4.22	3.06×10^{-1}	-1.60×10^{-4}	3.22×10^{-8}
nitrogen	31.15	-1.357×10^{-2}	2.681×10^{-5}	-1.168×10^{-8}

*Crystal diffusion parameters**	$\tilde{D}_{c,i} \approx D_{oc,i}\exp(-E_i/\Re T)$	
Component	$D_{oc,i}$, m^2/s	E_i, kJ/mol
propylene	5.8×10^{-8}	23.8
propane	1.4×10^{-8}	21.1

*Brandani et al. (1995).

The column is filled after 550 s during the adsorption step, while the blowdown is completed after 200 s. This defines the maximum values of these two steps to be introduced in the VSA with the feed flow shown in Table 3 and the maximum blowdown pressure range available with the experimental unit (0.1–5 bar).

Feed-pressure effect

Breakthrough experiments were carried out between 1.1 and 5 bar in order to verify the effect of pressure on the adsorption step and the influence of the initial pressure dur-

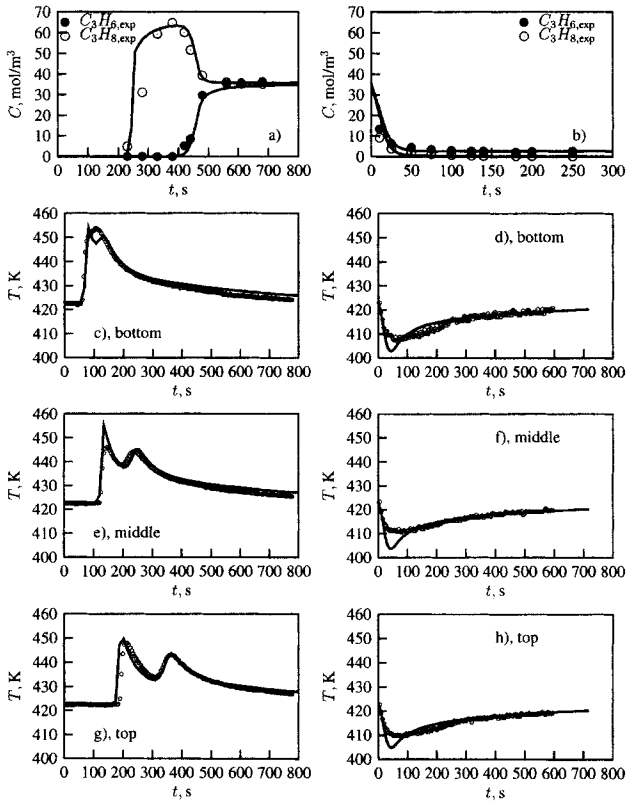

Figure 3. Experimental C_3H_6/C_3H_8 breakthrough and blowdown on 13X CECA zeolite, temperature histories at the bottom, middle and column top (a, c, e, and g), and during the blowdown (b, d, f, and h) for run G.

Solid lines are simulations with model shown in Table 1. Feed at 5 bar and 423 K.

ing the blowdown regeneration step. While Run D has the same feed characteristics and temperature as Runs A–C, it was carried out at lower pressure (1.1 bar). The breakthrough time is practically reduced to half when the feed pressure is reduced from 5 bar to 1.1 bar. Also the mole concentration is lower in the blowdown step as a result of starting the step at lower pressure after the feed step. The heat effects are reduced at a lower pressure operation, but the loading capacity of the column is reduced, too. The breakthrough time is reduced from 600 s to 400 s. This group of experiments allows us to define a period of time between 400 and 600 s to saturate the column at 423 K, limiting the high-pressure feed step to a period of time of less than 10 min with the volumetric flow rates defined in Table 3.

Figure 4a compares the breakthrough curves, and Figure 4b compares the temperature histories at the middle of the column for cases D, H, and G, where the feed pressure is 1.1, 2, and 5 bar, respectively. The effect of high-pressure feed during the adsorption step is clearly observed as an increase in concentration in the breakthrough concentration shown in Figure 4a and temperature peak size in Figure 4b. It is also observed that for the higher pressure feed, the first temperature peak becomes larger than the second peak, as seen in Figure 4b. While the total pressure of the feed increases from 1.1 to 5, the loading of the column increases, and more propylene is adsorbed from the feed compared with propane, changing the relative sizes of the first and second peaks. When the 5-bar pressure is reached, the energy released by the propylene adsorption, which has the higher isosteric heat of adsorption, equals the energy adsorbed by the propane being displaced, and the first peak becomes higher. During the blowdown step, the temperature minimum is lower when the step starts at high pressure (5 bar), and increases gradually while the initial pressure of the blowdown is reduced from 5 bar to 1.1 bar, as observed in Figure 4c. Again, the explanation of this fact is the reduction of the material loaded in the

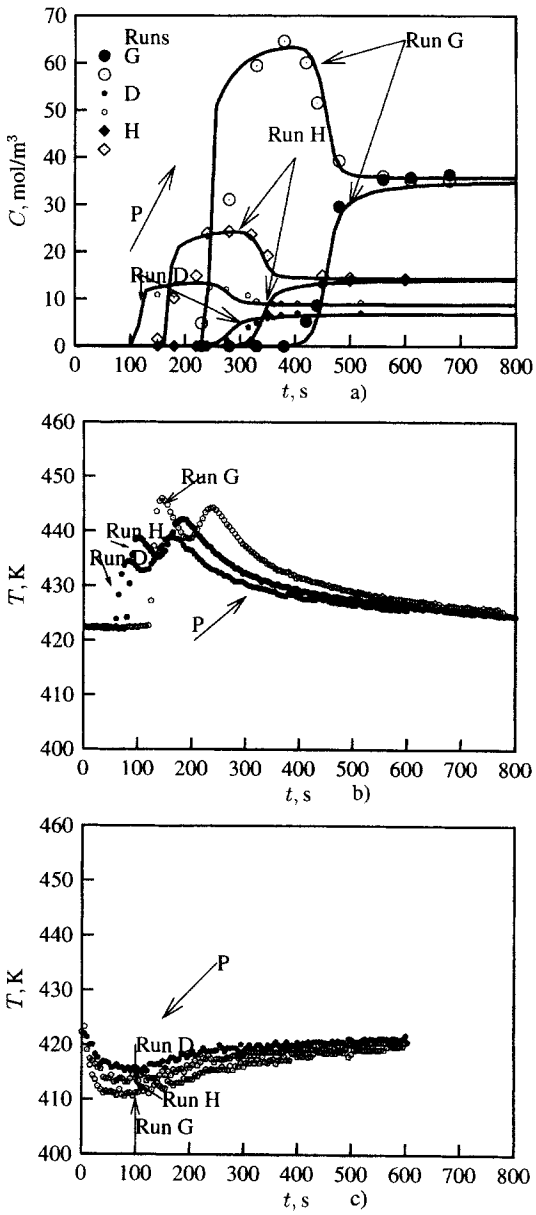

Figure 4. (a) Effect of the high-pressure feed on the breakthrough and (b) temperature histories at the middle of the column during the feed and (c) blowdown step.

Run D, 1.1 bar; Run H 2 bar; run G 5 bar.

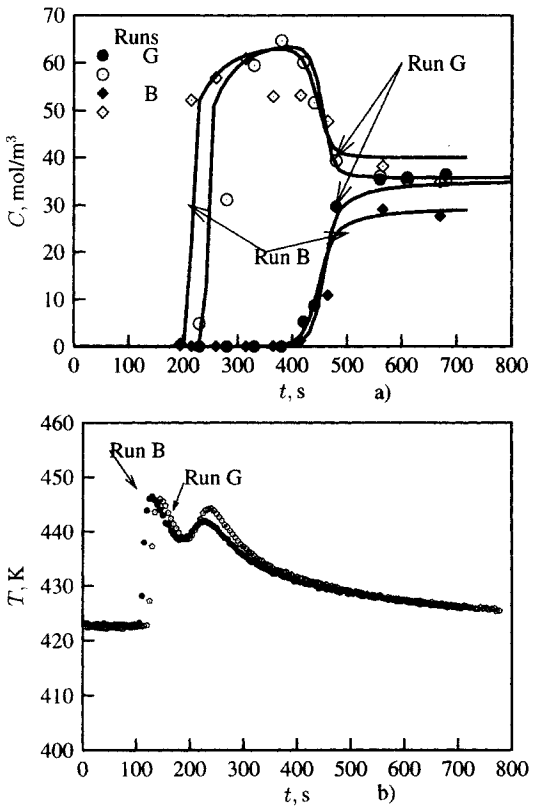

Figure 5. (a) Effect of feed mole composition on the breakthrough and (b) temperature histories at the middle of the column.

Run B, C_3H_8/C_3H_6 mole ratio 1.3; Run G, C_3H_8/C_3H_6 mole ratio 1. Temperature 423 K and pressure 5 bar.

column after it is saturated with feed while the pressure is lowered from 5 bar to 1.1 bar, diminishing the sorbate removed during the blowdown step, and so, decreasing the heat effects.

Feed-composition effect

Figure 5 compares the breakthrough (Figure 5a) and temperature histories at the middle of the column (Figure 5b) for experiments B and G, which were carried out with different propylene/propane relative mole ratios, ($y_{propane}/y_{propylene}$ = 1.3 in case B, to 1 in case G) and similar total volumetric flow (2–2.15 SLPM), feed pressure (5 bar), and temperature (423 K) during the high-pressure feed. The experiment with a large propane/propylene ratio (Run B) shows a wider breakthrough and temperature history at the central point of the column. Also, the first temperature peak for Run *B* is higher than for Run G, as shown in Figure 5b. These two results are expected, since more propane is being adsorbed in case B than in case G.

Temperature effect

The effect of temperature on the fixed-bed experiment is shown in Figure 6, where the breakthrough (Figure 6a) and temperature histories at the middle of the column are shown during the feed (Figure 6b) and blowdown (Figure 6c). Run I (at 393 K) is compared with Run G (at 423 K). In Figure 6a, the two breakthrough curves are compared where case I shows a slower response than case G. A larger tail is obtained at the end of the run, which reduces the separation efficiency and requires practically twice the time to saturate the column. A higher propane overshoot is also obtained and a higher first temperature peak during the high-pressure feed is recorded. These two results are directly supported by a more favorable isotherm for adsorption and the increment of the mass-transfer resistance, both at lower temperatures.

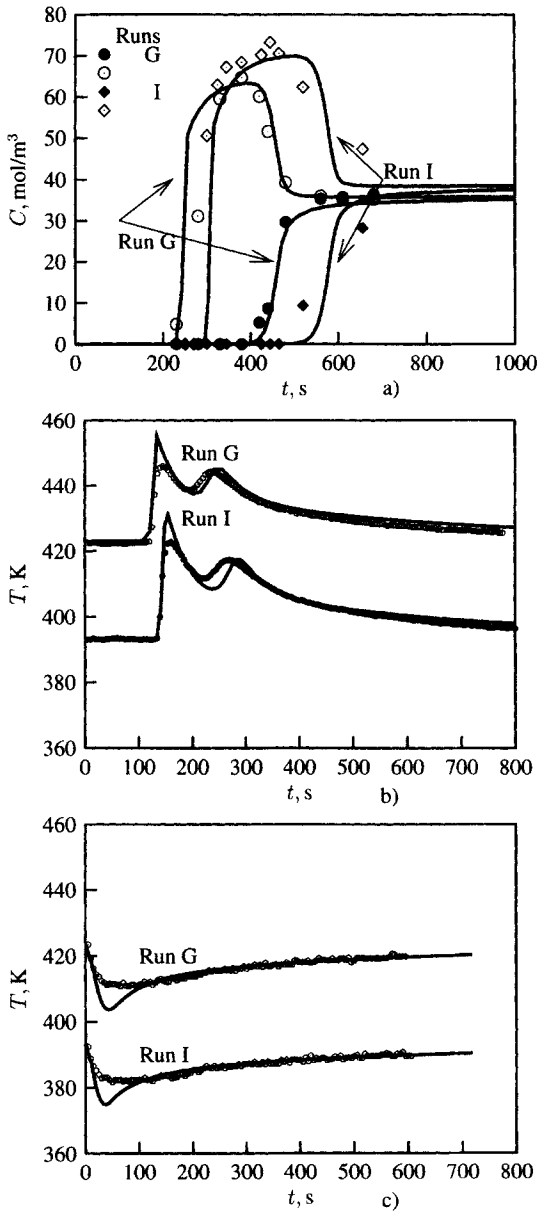

Figure 6. (a) Effect of the feed temperature on the breakthrough and temperature histories at the middle of the column during the (b) feed and (c) blowdown steps.

Run G at 423 K; Run I at 393 K.

Effect of the total feed volumetric flow

The effect of the total feed volumetric flow on the breakthrough and temperature history at the middle of the column can be observed in Figure 7, where Runs I and J (with half of the total volumetric flow) at 393 K and a total feed pressure of 5 bar are compared. As a direct consequence of decreasing the volumetric total flow to half in Run J, the breakthrough curve (Figure 7a) and temperature signal (Figure 7b) take nearly twice the time to appear. The direct reduction of the space time of the system through the reduction of the superficial velocity at the feed end explains these results. On the other hand, during the blowdown step, the temperature history at the middle of the column is identical in both cases, as confirmed in Figure 7c. This is obvious in the sense that equal initial conditions are found in the blowdown step for both cases, after complete saturation of the column with the equimolar propylene/propane feed at 423 K and 5 bar of total pressure.

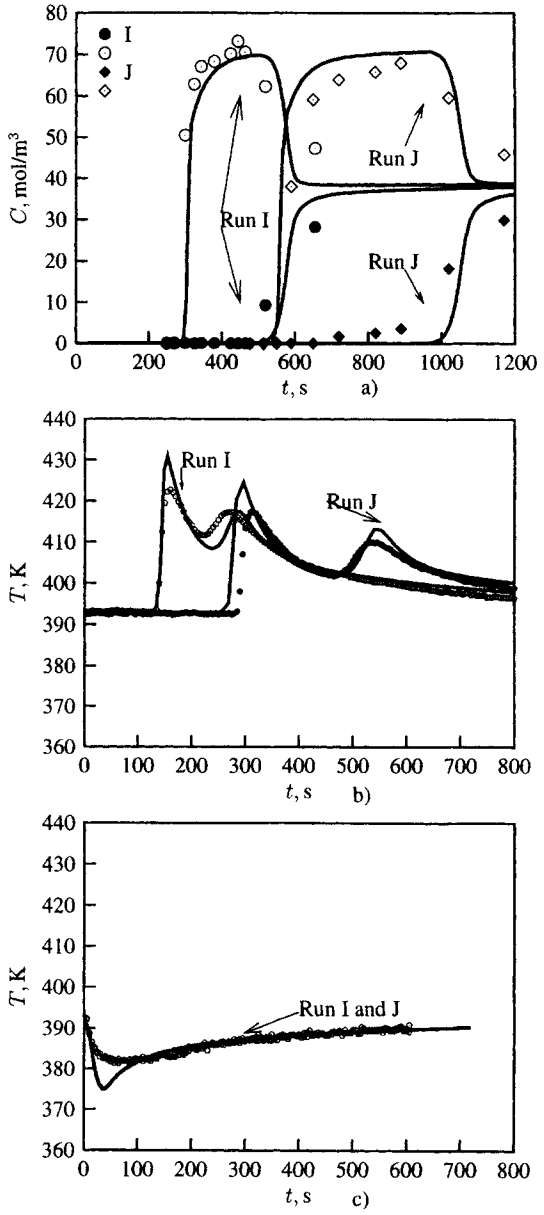

Figure 7. (a) Effect of total volumetric feed flow rate on the breakthrough and temperature histories at the middle of the column during the (b) feed (c) blowdown steps.

Run I, total flow 2 SLPM; Run J total flow 1 SLPM; both at 393 K and 5 bar total pressure.

VSA Results and Discussion

After the fixed-bed runs, a group of vacuum swing adsorption (VSA) experiments were carried out following the adsorption sequence shown in Figure 2. The contact time during the high-pressure feed at 5 bar and 423 K should be lower than 10 min, and the countercurrent blowdown should be carried out in no more than 200 s as a result of the fixed-bed experiments. This information was the initial point from which the VSA time steps were conceived.

Preliminary VSA experiments

Once the VSA steps are defined, a first group of the VSA experiments was carried out in order to set a range of operating conditions to obtain high-purity propylene product. Table 5 shows the main operating conditions, time used for the high-pressure feed and purge, and the performance of the experimental VSA runs. The blowdown time was fixed at 120 s (except for Run 6), supported by the results during the fixed-bed experiments, while the high-pressure blowdown time (from P_H to P_M) was fixed in 60 s for all experiments.

The pressurization and high-pressure feed were carried out with an equimolar propylene/propane stream diluted at 50% with nitrogen and a total flow of 2 SLPM for Runs 1–29; in case 30, the propylene/propane proportion in the feed stream was incremented by a factor of 4. The base operation temperature was fixed in 423 K, the maximum feed pressure in 5 bar, and the low pressure in the countercurrent blowdown step was fixed at 0.1 bar.

Runs 1–12 constituted the preliminary experiments. In Runs 1–4 the duration of the high-pressure feed was fixed at 300 s, and that of the high-pressure purge was set at 150 s. Within this set of experiments, the $P_M = 2$ bar was fixed, while the amount of propylene used to purge the column was changed. Run 1 gave zero recovery and productivity, meaning that 0.4 SLPM of propylene or the P/F ratio is too high for the feed introduced and the propylene obtained and should therefore be reduced. That is done in Run 2, where P/F was reduced to nearly half, leading to a propylene purity of 96% and a recovery of over 20%. At the extreme limit, the propylene is eliminated from the purge stream in run 3, using single nitrogen as the purge gas ($P/F = 0$ in terms of propylene introduced). For this case the purity is reduced from 96% to 91%. Because the objective of the VSA is to produce high-purity propylene, the last result indicates that part of the propylene produced should be used during the high-pressure purge. In Run 4 propylene was introduced again in the purge stream (0.1 SLPM of C_3H_6 + 3.6 SLPM of N_2 defining a $P/F \sim 0.1$ for propylene). This gives nearly 95% purity, as defined with Eq. 2, with higher productivity with respect to Run 2.

Table 5. VSA Experiments for the Separation of Propylene/Propane System Over 13X CECA Zeolite

Case	T K	P_{high} bar	P_{medium} bar	P_{low} bar	Pres. s	Feed s	Purge s	H-Blow s	L-Blow s	$Q_{C_3H_6}$ SLPM	Q_{N_2} SLPM	P/F	C_3H_6 Purity %	Recovery %	Productivity mol/kg·h
Run 1	423	5	2	0.1	60	300	150	60	120	0.4	3.6	0.343	96.0	0	0
Run 2	423	5	2	0.1	60	300	150	60	120	**0.19**	3.6	0.175	96.9	20.8	1.24
Run 3	423	5	2	0.1	60	300	150	60	120	**0**	3.6	0	91.8	19.7	1.45
Run 4	423	5	2	0.1	60	300	150	60	120	**0.1**	3.6	0.092	94.5	19.8	1.57
Run 5	423	5	2	0.1	60	**150**	150	60	120	0.1	3.6	0.163	95.9	33.0	1.46
Run 6	423	5	2	0.1	60	**300**	150	60	**180**	0.1	3.6	0.092	95.8	22.7	1.27
Run 7	423	5	2	0.1	60	**60**	150	60	120	0.1	3.6	0.296	96.1	48.6	1.42
Run 8	423	5	**1**	0.1	60	60	150	60	120	**0.1**	3.6	0.300	92.5	46.9	1.34
Run 9*	423	5	**0.5**	0.1	60	60	150	60	120	0.1	3.6	0.482	97.4	40.1	0.717
Run 10	423	5	0.5	0.1	60	60	150	60	120	0.1	**0**	0.278	74.8	54.5	1.69
Run 11	423	5	**0.2**	0.1	60	60	150	60	120	0.1	**3.6**	0.307	92.3	4.0	0.111
Run 12**	423	5	**0.5**	0.1	60	60	150	60	120	0.1	3.6	0.278	81.8	56.8	1.33
Run 13	423	5	0.5	0.1	60	**120**	**120**	60	120	**0.3**	3.6	0.440	98.0	19.2	0.785
Run 14	423	5	0.5	0.1	60	**120**	**120**	60	120	**0.3**	3.6	0.440	98.5	16.2	0.634
Run 15	**453**	5	0.5	0.1	60	120	120	60	120	0.3	3.6	0.445	98.0	4.2	0.171
Run 16	**393**	5	0.5	0.1	60	120	120	60	120	0.3	3.6	0.434	97.1	17.9	0.745
Run 17	423	5	0.5	0.1	60	120	120	60	120	**0.15**	**1.8**	0.224	90.9	33.7	1.408
Run 18	423	5	0.5	0.1	60	120	120	60	120	**0.1**	**1.2**	0.158	90.4	34.3	1.432
Run 19	423	5	0.5	0.1	60	120	120	60	120	**0.3**	**1.8**	0.431	94.6	26.1	1.090
Run 20	423	5	0.5	0.1	60	120	120	60	120	0.3	**1.2**	0.429	93.1	31.7	1.33
Run 21	423	5	0.5	0.1	60	120	120	60	120	0.3	**0.3**	0.423	91.5	25.5	1.09
Run 22	423	5	0.5	0.1	60	120	120	60	120	**0.15**	**3.6**	0.230	97.0	22.4	0.911
Run 23	423	5	0.5	0.1	60	120	120	60	120	**0.075**	3.6	0.136	94.8	18.6	0.759
Run 24	423	**3**	0.5	0.1	60	120	120	60	120	**0.3**	3.6	0.503	99.1	0	0
Run 25	423	**3**	0.5	0.1	60	120	120	60	120	**0.15**	3.6	0.261	97.4	6.7	0.239
Run 26	423	**1.5**	0.5	0.1	60	120	120	60	120	0.15	3.6	0.440	95.7	25.4	1.039
Run 27	423	**5**	**2**	0.1	60	120	120	60	120	**0.3**	3.6	0.440	95.7	25.0	1.036
Run 28	423	5	**1**	0.1	60	120	120	60	120	0.3	3.6	0.440	98.5	12.7	0.518
Run 29	423	5	1	0.1	60	120	120	60	120	**0.15**	**1.8**	0.227	94.3	30.5	1.26
Run 30†	423	5	0.5	0.1	60	120	120	60	120	**0.3**	**3.6**	0.275	99.3	12.5	0.822

*Pressurization with 5 SLPM N_2, 0.5 SLPM propylene, and 0.5 SLPM propane.
**Low-pressure blowdown replaced by a vacuum countercurrent purge with nitrogen, 0.1 SLPM at 0.1 bar during 120 s.
†Pressurization and feed steps with a stream of 0.8, 0.2, and 1.0 SLPM of propylene, propane, and nitrogen, respectively.

In order to improve the cycle, Runs 5 and 6 were carried out. In Run 5 the feed time was reduced in order to improve the productivity as a consequence of reducing the total cycle time (from cycle schedule pressurization 60 s + feed 300 s + high purge 150 s + high blowdown 60 s + vacuum blowdown 120 s = 690 s of run 4 to 540 s reducing the feed step time to half of run 5). The purity was kept at nearly 96% and the productivity at 1.46 mol/kg·h, but the recovery was increased from 20% to 33%. Run 6 was done in the same conditions as Run 4, but the vacuum blowdown time was increased from 120 to 180 s. The purity and recovery were improved marginally (from 94.5% to 95.8% and from 19.8% to 22.7%, respectively), but the productivity decreased because of the increase in the total cycle time from 690 to 750 s.

Plans were made from Runs 4 and 5 to further reduce the amount of feed introduced in the system, reducing further the feed step to 60 s. During Run 7, the purity was kept on 96.1% (compared to 94.5% for Run 4 or 96.9% for Run 2), but the recovery was practically doubled from 20% to 45%, which kept the productivity over 1.4 mol/kg·h.

The following steps in the preliminary runs were oriented to improve the purity by handling the pressure P_M. Run 8 was carried out with the same operating parameters as case 7, but reducing P_M from 2 bar to 1 bar, while in Run 9, P_M was reduced to 0.5 bar. In terms of the recovery, Run 8 was as effective as Run 7, where the feed time was reduced to 60 s, obtaining a recovery of over 40%; however, the purity (92.5%) was not improved as it was in case 8. Run 9, with $P_M = 0.5$, gave better purity (> 97%), but it cannot be fairly compared with Run 7, because during the pressurization step more N_2 was introduced (5 SLPM) than in Run 7 (1 SLPM). Although that experiment cannot be used for comparison, it indicates that the presence of nitrogen helps to improve the relative propylene/propane separation by reducing the partial pressure of the C_3H_6/C_3H_8 group.

Run 10 was carried out to explore the effect of nitrogen on the purity product in the VSA experiments. The nitrogen was eliminated from the high-pressure purge during that run. In spite of that, propylene recovery was one of the highest so far (> 50%), the purity obtained being the worst (75%). While nitrogen is present in the system, the partial pressure of the C_3 group is lower and the desorption is enhanced during the purge and the blowdown steps.

Run 11 was done with conditions similar to those in Run 7, but $P_M = 0.2$ and taking care of performing the pressurization with the same nitrogen flow. It is observed that purity was not improved, and the recovery strongly dropped (a low 4% recovery was obtained). This result establishes that the

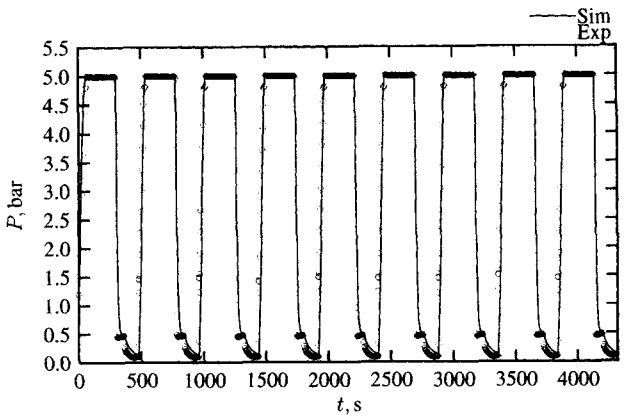

Figure 8. Simulated and experimental history pressure at the exit end of the VSA process (Run 13).

lower values of P_M (as low as 0.2 bar) do not further improve the purity of the product, but reduces the performance of the system both in terms of recovery and productivity.

Finally, Run 12 was carried out. During this test, the countercurrent blowdown step was replaced by a vacuum countercurrent purge step, with nitrogen at 0.1 bar and 0.1 SLPM for 120 s. The highest recovery of all the experimental sets was obtained in this run (56.8%), but the purity was not good (81.8%). Also, the product obtained was further diluted with inert gas that should be avoided.

Understanding the basic steps of the VSA process

In this subsection we consider the basic steps of the VSA process, comparing experimental results with simulation using the model shown in Table 1 and following the VSA sequence defined in Figure 2. Figures 8–10 show the main experimental results and simulated values with SAXS for Run 13 (Table 5). Figure 8 shows the pressure history at the feed end of the column compared with the pressure history obtained with the SAXS simulator. Both curves agree fairly well. The pressurization is carried out during the first 60 s, where

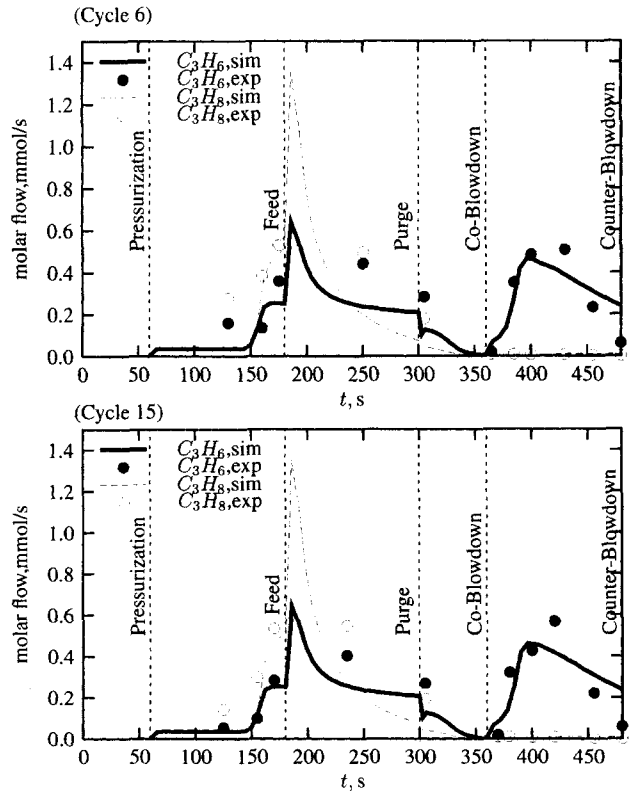

Figure 9. Simulated and experimental molar flow of propylene and propane at the (a) exit end of the VSA process during cycle 6 and (b) cycle 15 in cyclic steady state operation, Run 13.

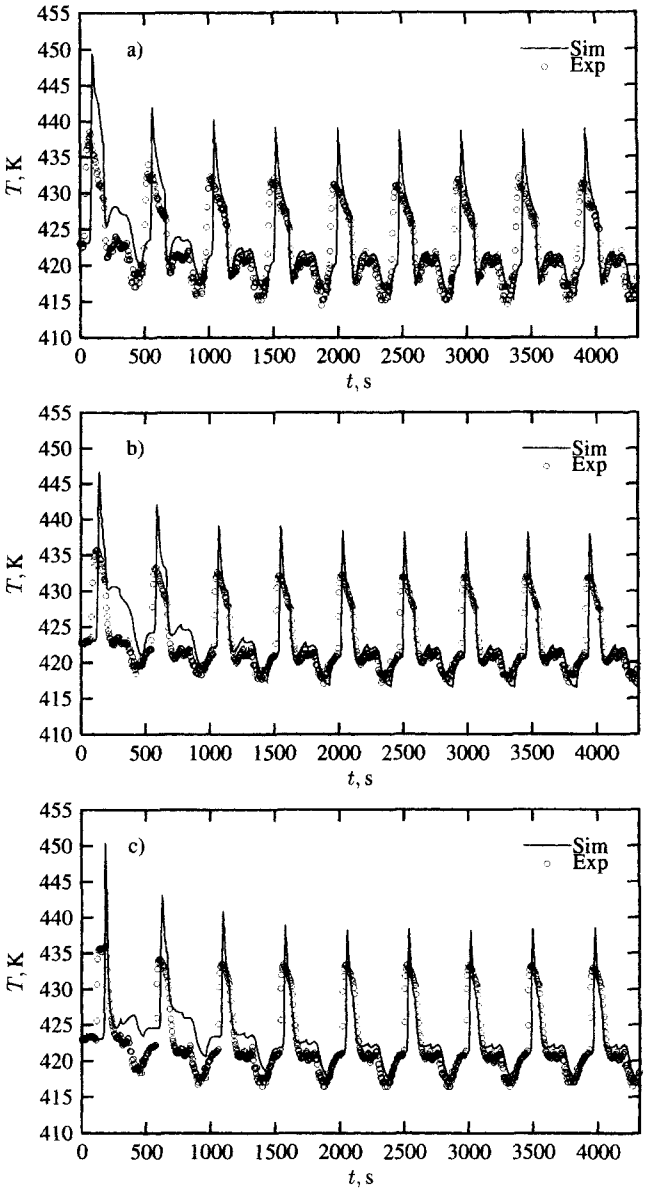

Figure 10. Simulated and experimental temperature measured at 0.2 m of the (a) feed end, (b) center and (c) 0.2 m below the top of the column during the VSA process (Run 13).

the pressure raises from the low-vacuum pressure of 0.1 bar to 5 bar, which is the high-pressure feed of this system. In the first cycle, however, the initial pressure is 1.2 bar, when the column is filled with nitrogen at the beginning of the experiments. Then follow the high-pressure feed (120 s) and the high-pressure purge (120 s), where the pressure is kept at 5 bar. The pressure is reduced to 0.5 bar during the high-pressure blowdown, and finally the pressure is further reduced to 0.1 bar in the low-pressure countercurrent blowdown step. After the first cycle, the pressure history along the cycle is repeated, cycle by cycle, until the other operating variables achieve the cyclic steady-state condition.

Figure 9 shows the evolution of the molar flow of propylene and propane from cycle 6 to cycle 15 compared with the numerical simulation obtained with the SAXS. The experimental results and numerical simulation do not agree perfectly. It should be noticed that the numerical simulation follows the experimental response and the total amounts of propylene and propane exiting from each step are very similar if the areas below the curves are compared. The difference between the experimental and simulation curves is mainly due to the average nature of the experimental value and the instantaneous origin of the numerical results. While the samples are carried out for at least 5 s or more, the simulated runs are instantaneous values exiting the column. For this reason, the experimental and simulated performance characterization of the VSA process through purity, recovery, and productivity are in better agreement, as shown later, because both are integral values calculated from a complete cycle.

Also the experimental values obtained from the experimental unit are affected by the dynamics of the back pressure, the vacuum pump that works during the blowdown steps, and the multivalve system when the sample is trapped, while in the numerical simulation the values computed are the ones obtained at the feed end of the column without the interference of other equipment. Consequently, larger differences are expected when switching from one step to another in the experimental curve compared with the simulated curve after each step change. The experimental results show the same profile from cycle 6 to 15, which means that the apparent cyclic steady-state condition is achieved in a few cycles.

The temperature evolution is observed at three different locations (at 20, 40, and 60 cm of the feed end) in Figures 10a to 10c. After a brief evolution of the temperature in the first five cycles, the temperature history at the three positions stabilizes around a cyclic steady-state behavior. The numerical results agree fairly well with the experimental points, presenting larger discrepancies at the first cycle. The main differences are found here because after regeneration the real column always lost a small amount of its capacity, while the simulations are computed assuming a perfectly clean column as an initial condition. After loading the column during the first five cycles, the numerical and experimental results agree better when the column is partially loaded with propylene and the cyclic steady state is approached.

Figures 11, 12 and 13 show the axial profile of the mole fraction, adsorbed phase concentration, temperature, and superficial velocity along a complete cyclic steady state. Figures 11 and 12 show that two mass-transfer zones move toward the exit end during the feed step. It is clearly shown that only

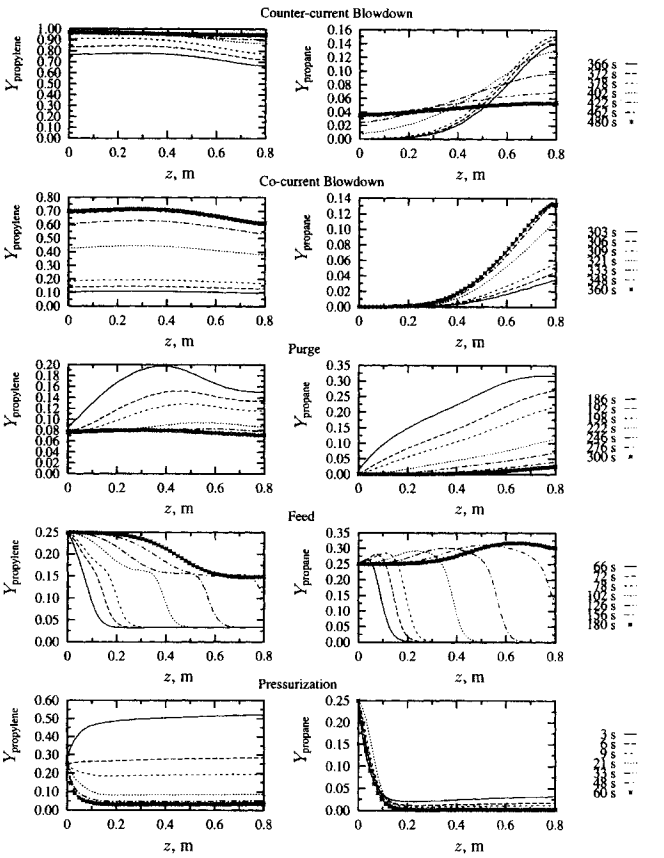

Figure 11. Propylene and propane mole fraction evolution during each step vs. axial distance z along a complete steady-state cycle (Run 13).

one mass-transfer zone leaves the column and that the second one is kept in the column. During this step, the column is saturated half way with fresh feed.

The purge step eliminates the propane. As can be seen from Figures 11 and 12, nearly 90% of the propane is eliminated from the column while the amount of propylene stored in the column is kept almost constant.

The cocurrent blowdown follows the purge, where the propylene mole fraction increases nearly 10 times, while the propane is kept low, especially at the feed end, as observed in Figure 11. However, in Figure 12 reduction of the amount of adsorbed propylene and propane is low. The increase in the propylene and propane mole fractions during this cocurrent blowdown is mainly due to the withdrawal of the inert gas from the system. This result is further supported by Figure 13. During the cocurrent blowdown step, the temperature variation is kept within 1–2 K, while in the countercurrent, blowdown is higher than 7 K. Without this step, the propylene obtained in the next step will be diluted with nitrogen.

The last step is the countercurrent blowdown, where high-purity propylene is obtained. Figures 11 and 12 show that practically 99% propylene mole fraction is obtained at the end of this step. However, because of the small amount of propane that still remains in the column, the ideal 99.9+% is difficult to obtain.

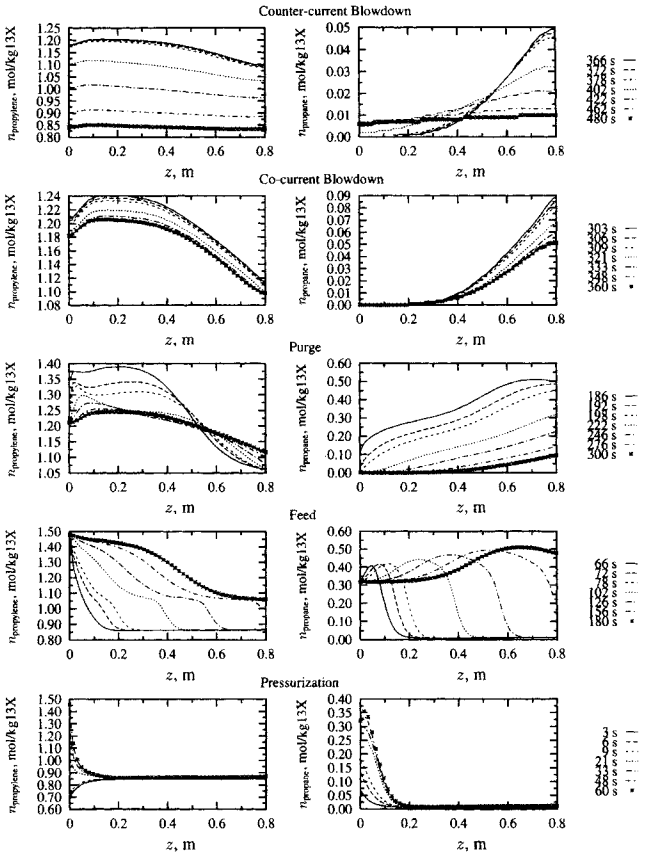

Figure 12. Evolution of axial profiles of propylene and propane adsorbed-phase concentration for each step along a complete steady-state cycle (Run 13).

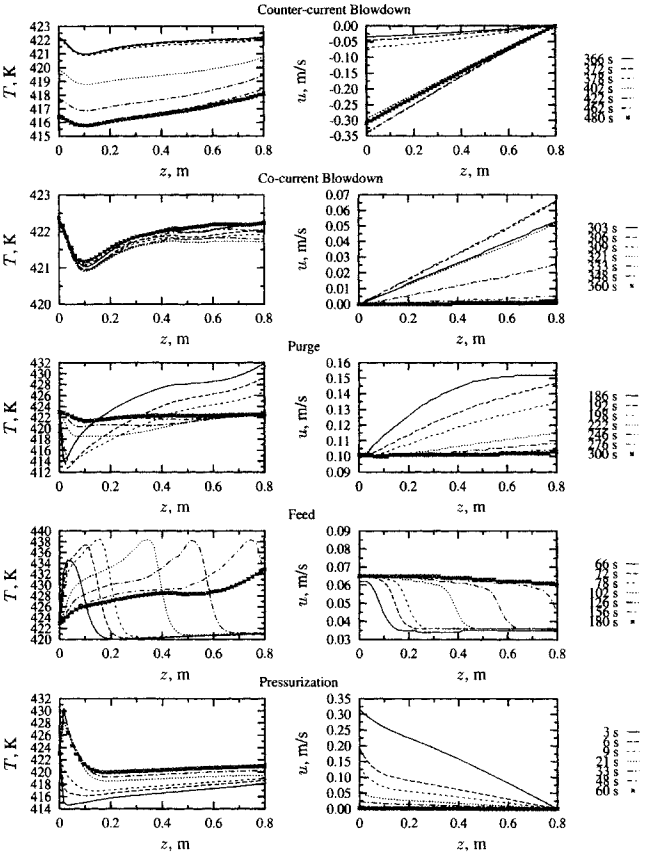

Figure 13. Evolution of temperature and superficial-velocity axial profiles for each step along a complete steady-state cycle (Run 13).

Effect of the operating temperature

Figure 14a summarizes the main results obtained from the VSA experiments that were carried out at three temperature levels: 393, 423 and 453 K. The performance values are taken from Table 5, Runs 13, 15, and 16. At the highest temperature the productivity and recovery are reduced while the purity is maintained at over 97% (see Eqs. 2–4). The reduction in productivity/recovery is caused by the reduction in the loading capacity of the column when the temperature increases, and therefore by the reduction in the material extracted from the column during the blowdown vacuum step. Table 6 shows a small reduction in the amount of nitrogen in the product, that is, between 1 and 5%. At lower temperatures, nitrogen is more concentrated in the column, and it is more difficult to eliminate it during the high-pressure blowdown, compared with the higher temperature case, keeping the same operating parameters. A temperature of 423 K appears to be adequate to obtain high purity, productivity, and recovery with a low amount of nitrogen in the product.

Effect of the intermediate blowdown pressure on the performance of VSA with 13X zeolite

Figure 14b shows the effect of the intermediate pressure on the performance of the VSA process. At lower pressures, the product purity is high and the productivity–recovery values decrease. This is a direct result of two facts: (1) a further reduction in the intermediate pressure allows more material to be withdrawn from the column before the final counter-current blowdown step, reducing the productivity–recovery of the process; and (2) allowing some of the propane exiting during the high-pressure blowdown avoids its appearance in the production step and increasing the relative purity of the propylene. The nitrogen in the product is also reduced.

Effect of the high-pressure feed on the performance of VSA

The effect of the feed pressure is shown in Figure 14c, where the results of Runs 22, 25, and 26 and compared. While

Table 6. Amount of Nitrogen in Molar Percentage in Propylene Product

Run	% N_2	Run	% N_2
13	3.2	**22**	< 1
14	3.2	**23**	10.5
15	1.1	**24**	9.7
16	5.5	**25**	10.6
17	5.2	**26**	71.8
18	2.7	**27**	16.8
19	2.3	**28**	8.2
20	1.5	**29**	7.1
21	< 1	**30**	< 1

the feed pressure rises from 1.5 bar to 5 bar, the purity of the propylene increases, too, as a direct result of more propylene being adsorbed relative to propane and then released in the product. The recovery is reduced at the same time that the nitrogen concentration in the product is reduced (see Table 6). At lower feed pressure the isotherm is more favorable to desorption of propylene, and it is more effectively recovered as product. At 3 bar the recovery is too low. Reviewing Table 5 for Runs 24 and 25, with both experiments fed at 3 bar, a null recovery for Run 24 is obtained, while only 6.7% is recovered for Run 25. The purge used during Run 24 is too high, resulting in 99% product purity but not productivity (all propylene product is used to purge the column). From this result, the purge feed in Run 25 was reduced by a half, obtaining a reduced purity of 97.4%, but a recovery of 6.7%. Experiment 26 was carried out with the same purge rate at 1.5 bar of total pressure, and a higher recovery of 25.4%, but a lower purity of 95.7%, were obtained. The increment of recovery is related to the fact that a lower amount of feed is required in the pressurization step, while during the production step a similar amount of propylene is obtained in both cases, but with lower purity at low pressure. At 5 bar the column is further loaded, and the recovery product increases again, but with higher purity with respect to 1.5 bar.

Effect of the purge-to-feed ratio in the performance of VSA with 13X zeolite

The effect of the *P/F* mole ratio is shown in Figure 14d, where the total amount of purge stream is varied and the mole composition is kept constant (0.077 mole fraction of propylene plus 0.923 mole fraction of nitrogen in Runs 13, 17, and 18) at a fixed flow feed (0.5 SLPM of propylene, 0.5 SLPM of propane, and 1 SLPM of nitrogen). At the highest *P/F* ratio, a higher-purity-enriched propylene product is obtained, but the recovery and productivity of the VSA process are reduced to half. A higher *P/F* ratio at constant feed forces the propylene/propane mass-transfer zone to travel further into the column, far from the production end, during the vacuum countercurrent blowdown. This enhances the propylene purity, because the contaminating propane is pushed further toward the opposite end.

Effect of nitrogen and propylene feed flow during high-pressure purge on the performance of VSA with 13X zeolite

Figure 14e shows the effect of increasing the nitrogen flow at constant propylene flow (0.3 SLPM) during the high-pressure purge step (Runs 13, 19 and 21). As shown by Figure 14e, the relative propylene/propane mole ratio increases when the amount of nitrogen is used in the high-pressure purge step, but the amount of nitrogen in the product also is increased, as observed in Table 6. While more inert gas is used during the high-pressure purge step, the better will be the regeneration in both blowdown steps, but the recovery and productivity decrease because more material is removed from the column in the purge step.

Figure 14f shows the effect of high-pressure propylene purge gas keeping the nitrogen flow constant in 3.6 SLPM (Runs 13, 22 and 23). Similarly, as the propylene concentration in the purge stream is increased, the product purity also increases, while the nitrogen concentration in the product is

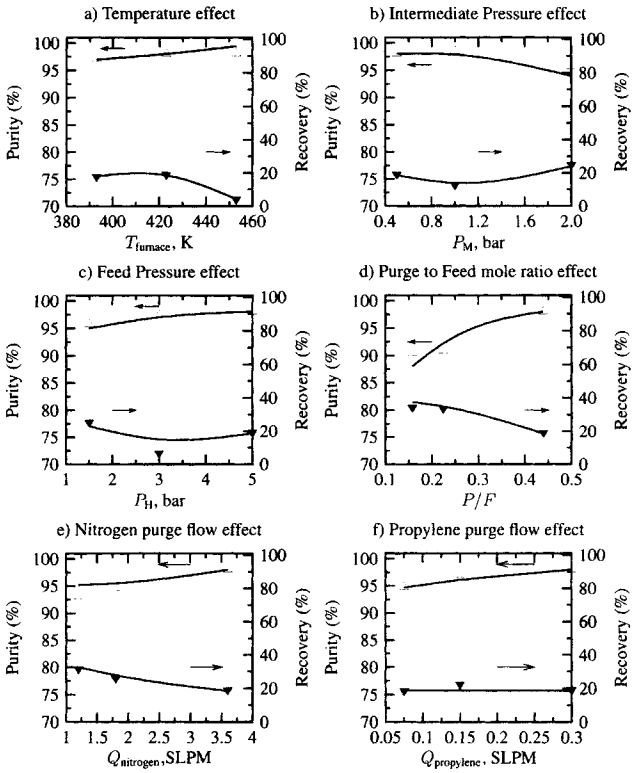

Figure 14. Effect of the operating parameters on the VSA performance, using 13X zeolite as sorbent.

(a) Temperature T; (b) intermediate pressure P_M; (c) feed pressure P_H; (d) purge/feed ratio P/F; (e) nitrogen-purge flow rate $Q_{nitrogen}$; (f) propylene-purge flow rate $Q_{propylene}$.

reduced. The recovery and productivity values are between 18 and 22 and 0.76 and 0.91 (see Table 5), which is too narrow a variation to be considered an important effect. This means that increasing the propylene flow from 0.075 SLPM to 0.3 SLPM, and keeping the other operating parameters constant does not affect significantly the productivity and recovery values, but improves the purity of the propylene product. After the high-pressure feed, the column is saturated, and during the purge step, the recycled fresh propylene mainly cleans the void space of the column, keeping the loaded amount of propylene in the solid phase almost constant, preparing the column for the production step. However, increasing the amount of propylene used during the purge step further will strongly reduce the productivity and recovery.

Conclusions

Experimental fixed-bed and vacuum swing adsorption (VSA) experiments were shown for the propylene/propane separation using 13X CECA zeolite pellets. The fixed bed was loaded in 400–600 s, at 5 bar and 423 K, with a 2 SLPM of an equimolar propylene/propane mixture diluted by 50% with nitrogen, while the countercurrent blowdown from 5 bar to 0.1 bar took between 120 and 200 s. These adsorption/regeneration time steps defined the workable range of operation of the column for the pressurization, high-pressure feed,

and countercurrent blowdown steps of the VSA investigated. The effect of feed pressure, feed mole composition, operation temperature, and the total flow feed on the fixed-bed runs were shown.

Based on the breakthrough/blowdown experiments, a five-step VSA was designed for the propylene/propane separation, with the objective of producing high-purity propylene as follows. (1) *Pressurization with feed, 60 s:* The pressure is increased from the lower pressure P_L (0.1 bar), to the maximum pressure P_H (5.0 bar), with 2 SLPM, 25% propylene, 25% propane, and 50% nitrogen, from the bottom to the top of the column. (2) *High Pressure feed, 120 s:* In this step, the feed is kept at the higher pressure P_H, entering the column at 2 SLPM for 120 s. The bed accumulates propylene in the solid phase and an enriched propane stream diluted with nitrogen is produced. (3) *High-pressure purge with product, 120 s:* Part of the product is compressed, recycled, diluted with nitrogen, and introduced again in the column from the bottom to the top. This step is to improve the propylene purity of the product, but at the cost of lowering the recovery of the overall system. A prepared feed of 0.3 SLPM of propylene and 3.6 SLPM of nitrogen at 5 bar is introduced in this step. (4) *High-pressure cocurrent blowdown, 60 s*: During this step the column pressure is lowered to an intermediate pressure P_M (0.5 bar). This step further enriches the gas phase, with propylene being desorbed from the solid phase, and removes the excess nitrogen and some propane remaining in the column. (5) *Low-pressure countercurrent blowdown, 120 s*: The pressure is reduced further from the intermediate pressure P_M to the lower pressure P_L in the countercurrent flow. This is the production step, where high-purity propylene is obtained.

The 5-step VSA proposed to separate propylene/propane was investigated by experimentation and simulation. The column packed with 13X CECA pellets produced an enriched propylene stream with a purity of 98%, recovery of 19%, and productivity of 0.785 mol/kg·h. The cyclic steady-state condition was achieved in no more than 15 cycles. The bidisperse mass-transfer model implemented in SAXS followed the main behavior of the fixed-bed and VSA experiments. The effect of different operating parameters on the performance of the VSA, such as operating temperature, intermediate pressure, high-pressure feed, *P/F* mole ratio, and high-pressure purge flow, was analyzed. The temperature range between 393 K and 423 K presents the better results in terms of purity/recovery. The performance of the VSA cycle investigated was better at a higher total pressure of 5 bar, while the intermediate pressure between 0.5 and 1 bar achieved the best results. The *P/F* ratio between 0.3 and 0.4 guarantees purities higher than 95%, while the nitrogen and propylene are kept between 1 and 3.6 and 0.15 and 0.4 SLPM, respectively.

Acknowledgments

Financial support from PRAXIS XXI/3/3.1/CEG/2644/95 is gratefully acknowledged. F. A. Da Silva acknowledges research fellowship from PRAXIS XXI/BD5772/95.

Notation

a = pellet-specific area, m^{-1}
$Bi_{m,i}$ = mass Biot number
$\bar{c}_i$ = average concentration of i component in the pellet, mol/m^3
C_i = concentration of i component in the bulk, mol/m^3
$\hat{C}_{ps}$ = solid heat capacity, J/kg·K
$\hat{C}_{pw}$ = wall heat capacity, J/kg·K
$\tilde{C}_p, \tilde{C}_v$ = heat capacity at constant pressure and volume of the gas mixture, J/mol·K
d_p = pellet diameter, m
$\bar{D}_{c,i}$ = crystal diffusion coefficient for i component, m^2/s
$\bar{D}_{p,i}$ = pore diffusivity for i component, m^2/s
$D_{zm,i}$ = mass axial dispersion coefficient for i component, m^2/s
h_f = film heat-transfer coefficient between gas and solid, $W/m^2 \cdot K$
h_w = film heat-transfer coefficient between gas and the wall, $W/m^2 \cdot K$
$-\Delta H_i$ = isosteric heat adsorption of the i component, J/mol
k = equilibrium heterogeneity parameter
L = length of fixed bed, m
m = loading saturation parameter, mol/kg
$\bar{\bar{n}}_i$ = average adsorbed concentration for i component in the pellet, mol/kg
n_i^* = adsorbed phase concentration in the crystal in equilibrium with the gas inside the particle, mol/kg
P = gas pressure, kPa
P_H = high feed/purge pressure, kPa
P_L = low vacuum pressure, kPa
P_M = intermediate pressure, kPa
Pr = Prandtl number
$\Re$ = ideal gas constant (= 8.3144), J/mol·K
Re = Reynolds particle
Sc = Schmidt number
t = time, s
T = temperature, K
u = superficial gas velocity, m/s
U = overall heat-transfer coefficient, $W/m^2 \cdot K$
Y_i = mole fraction of i component in the bulk
z = axial position, m

Greek letters

α_w = ratio of the internal surface area to the volume of the column wall, m^{-1}
$\alpha_{w\ell}$ = ratio of the log mean surface to the volume of the column wall, m^{-1}
λ = heat axial-dispersion coefficient, $W/m^2 \cdot K$
ϵ = interparticle void fraction of bed
ϵ_p = pellet void fraction
ρ_p = pellet density, kg/m^3
ρ_w = wall density, kg/m^3

Superscripts and subscripts

$*$ = equilibrium
$\circ$ = pure component
$-$ = volumetric average
$=$ = double volumetric average
$\sim$ = per mol
$\wedge$ = per kilogram
c = crystal
g = gas
h = heat
i, j = i or j component
m = mass
p = pellet; constant pressure
s = solid
v = constant volume
w = wall
z = axial coordinate
∞ = ambient

Literature Cited

Brandani, S., J. Hufton, and D. Ruthven, "Self-Diffusion of Propane and Propylene in 5A and 13X Zeolite Crystals Studied by the Tracer ZLC Method," *Zeolites*, **15**, 624 (1995).

Carey, G. F., and B. A. Finlayson, "Orthogonal Collocation on Finite Elements," *Chem. Eng. Sci.*, **30**, 587 (1975).
Costa, E., G. Calleja, A. Jimenez, and J. Pau, "Adsorption Equilibrium of Ethylene, Propane, Propylene, Carbon Dioxide, and Their Mixtures on 13X Zeolite," *J. Chem. Eng. Data*, **36**, 219 (1991).
Da Silva, F. A., *Cyclic Adsorption Processes: Application to Propane/Propylene Separation*, PhD Thesis, Faculdade de Engenharia, Universidade do Porto, Porto, Portugal (1999).
Da Silva, F. A., M. E. Macedo, and A. E. Rodrigues, "Computer Aided Process Design and Optimization with Novel Separation Process," Tech. Rep., JOU2-CT93-0337, Final Report (Jan.–July, 1996).
Da Silva, F. A., and A. E. Rodrigues, "Adsorption Equilibria and and Kinetics for Propylene and Propane over 13X and 4A Zeolite Pellets," *Ind. Eng. Chem. Res.*, **38**, 2051 (1999a).
Da Silva, F. A., and A. E. Rodrigues, "A General Package for the Simulation of Cyclic Adsorption Processes," *Adsorption*, **5**, 229 (1999b).
Eldridge, R. B., "Olefin/Paraffin Separation Technology: A Review," *Ind. Eng. Chem. Res.*,. **32**(10), 2208 (1993).
Finelt, S., "Better C_3 Distillation Pressure," *Hydrocarbon Process.*, 95 (1979).
Ghosh, T. K., H.-D. Lin, and A. L. Hines, "Hybrid Adsorption-Distillation Process for Separating Propane and Propylene," *Ind. Eng. Chem. Res.*, **32**, 2390 (1993).
Howat, C. S., and G. W. Swift, "A New Correlation of Propene–Propane Vapor–Liquid Equilibrium Data and Application of the Correlation to Determine Optimum Fractionator Operating Pressure in the Manufacture of Polymerization-Grade Propene," *Ind. Eng. Chem. Process Des. Dev.*, **19**, 318 (1980).
Huang, Y.-H., J. W. Johnson, A. I. Liapis, and O. K. Crosser, "Experimental Determination of Binary Equilibrium Adsorption and Desorption of Propane-Propylene Mixtures on 13X Molecular Sieves by a Differential Sorption Bed System and Investigation of their Equilibrium Expressions," *Sep. Technol.*, **4**, 156 (1994).
Järvelin, H., and J. R. Fair, "Adsorptive Separation of Propylene-Propane Mixtures," *Ind. Eng. Chem. Res.*, **32**, 2201 (1993).
Kikkinides, E. S., R. T. Yang, and S. H. Cho, "Concentration and Recovery of CO_2 from Flue Gas by Pressure Swing Adsorption," *Ind. Eng. Chem. Res.*, **32**, 2714 (1993).
Kubota, K., K. Nakajima, Y. Ono, and S. Hayashi, "Adsorption Characteristics of Propylene on Molecular Sieve 4A," *Sep. Sci. Technol.*, **24**, 709 (1989).
Kulvaranon, S., M. E. Findley, and A. I. Liapis, "Increased Separation by Variable-Temperature Stepwise Desorption in Multicomponent Adsorption Process," *Ind. Eng. Chem. Res.*, **29**, 106 (1990).
Kumar, R., T. C. Golden, T. R. White, and A. Rokicki, "Novel Adsorption Distillation Hybrid Scheme for Propane/Propylene Separation," *Sep. Technol.*, **15**, 2157 (1992).
Loughlin, K. F., M. A. Hasanain, and H. B. Abdul-Rehman, "Quaternary, Ternary, Binary, and Pure Component Sorption on Zeolites. 1. Light Alkanes on Linde S-115 Silicate at Moderate to High Pressures," *Ind. Eng. Chem. Res.*, **29**, 1525 (1990).
Lu, Z. P., J. M. Loureiro, M. LeVan, and A. E. Rodrigues, "Simulation of a Three-Step One-Column Pressure Swing Adsorption Process," *AIChE J.*, **39**, 1483 (1993).
Manley, D. B., and G. W. Swift, "Relative Volatility of Propane-Propene System by Integration of General Coexistence Equation," *J. Chem. Eng. Data*, **16**, 301 (1971).
Netzer, D., "Economically Recover Olefins from FCC Offgases," *Hydrocarbon Process.*, 83 (1997).
Padin, J., and R. T. Yang, "Tailoring New Adsorbents Based on π-Complexation: Cation and Substrate Effects on Selective Acetyl ene Adsorption," *Ind. Eng. Chem. Res.*, **36**, 4224 (1997).
Ramachandran, R., L. H. Dao, and B. Brook, "Method of Producing Unsaturated Hidrocarbons and Separating the Same from Saturated Hydrocarbons," U.S. Patent No. 5,365,011 (1994).
Ramachandran, R., L. H. Dao, and B. Brook, "Process for Recovering Alkenes from Cracked Hydrocarbon Streams," U.S. Patent No. 5,744,687 (1998).
Rege, S. U., J. Padin, and R. T. Yang, "Olefin/Paraffin Separations by Adsorption: π-Complexation vs. Kinetic Separation," *AIChE J.*, **44**, 799 (1998).
Ruthven, D. M., *Principles of Adsorption and Adsorption Processes*, Wiley, New York (1984).
Schiesser, W. E., *The Numerical Method of Lines*, Academic Press, San Diego (1991).
Seery, M. W., "Bulk Separation of Carbon Dioxide from Methane using Natural Clinoptilolite," U.S. Patent No. 5,938,819 (1999).
Sherred, J. A., and J. R. Fair, "High Purity Propylene—A New Problem," *Ind. Eng. Chem.*, **51**, 249 (1959).
Sikavitsas, V. I., R. Yang, M. Burns, and E. Langenmayr, "Magnetically Stabilized Fluidized Bed for Gas Separations: Olefin-Paraffin Separations by π-Complexation," *Ind. Eng. Chem. Res.*, **34**, 2873 (1995).
Sircar, S., "Separation of Methane and Carbon Dioxide Gas Mixtures by Pressure Swing Adsorption," *Sep. Sci. Technol.*, **23**, 519 (1988).
Sircar, S., "Role of Adsorption Heterogeneity on Mixed Gas Adsorption," *Ind. Eng. Chem. Res.*, **30**, 1032 (1991).
Smuck, W. W., "Operating Characteristics of a Propylene Fractionation Unit," *Chem. Eng. Prog.*, **59**, 64 (1963).
Summers, D. R., P. J. McGuire, M. R. Resetarits, C. E. Graves, S. E. Harper, and S. J. Angelino, "High-Capacity Trays Debottleneck Texas C_3 Splitter," *Oil & Gas J.*, 45 (1995).
Tyreus, B. D., and W. L. Luyben, "Two Towers Cheaper than One?" *Hydroc. Process.*, 93 (1975).
Villadsen, J., and M. L. Michelsen, *Solution of Differential Equation Models by Polynomial Approximation*, Prentice-Hall, Englewood Cliffs, NJ (1978).
Wakao, N., and T. Funazkri, "Effect of Fluid Dispersion Coefficients on Particle-to-Fluid Mass Transfer Coefficients in Packed Beds," *Chem. Eng. Sci.*, **33**, 1375 (1978).
Wiessner, F. G., "Basics and Industrial Applications of Pressure Swing Adsorption (PSA), the Modern Way to Separate Gas," *Gas Sep. Purif.*, **2**, 115 (1988).
Yang, R. T., *Gas Separation by Adsorption Processes*, Butterworths, Boston (1987).
Yang, R. T., and E. S. Kikkinides, "New Sorbents for Olefin/Paraffin Separations by Adsorption Via π Complexation," *AIChE J.*, **41**, 509 (1995).
Yang, R. T., E. S. Kikkinides, and R. Foldes, "New Sorbents for Olefin-Paraffin and Acetylene Separations by π-Complexation," *Fundamentals of Adsorption*, M. LeVan, ed., Kluwer, Boston, p. 1047 (1996).

Manuscript received Apr. 5, 2000 and revision received June 27, 2000.